The relationship between interface structure, conformality and perpendicular anisotropy in CoPd multilayers

2005 J. Phys.: Condens. Matter 17 3759

(http://iopscience.iop.org/0953-8984/17/25/004)

INSTITUTE OF PHYSICS PUBLISHING JOURNAL OF PHYSICS: CONDENSED MATTER

J. Phys.: Condens. Matter **17** (2005) 3759–3770 doi:10.1088/0953-8984/17/25/004

The relationship between interface structure, conformality and perpendicular anisotropy in CoPd multilayers

A S H Rozatian[1,3], C H Marrows[2], T P A Hase[1] and B K Tanner[1]

[1] Department of Physics, University of Durham, South Road, Durham DH1 3LE, UK
[2] School of Physics and Astronomy, University of Leeds, Leeds LS2 9JT, UK

Received 9 March 2005, in final form 18 May 2005
Published 10 June 2005
Online at stacks.iop.org/JPhysCM/17/3759

Abstract

The relationship between the interface structure and perpendicular anisotropy in sputtered Co/Pd multilayers has been investigated using grazing incidence x-ray scattering and vibrating sample magnetometry. Using fits to a self-affine fractal model of the interfaces, the variation in in-plane correlation length, fractal parameter and conformality has been determined as a function of the number of repeats in the Co/Pd bilayers. As the number of interfaces rises, the roughness becomes predominantly non-conformal and the in-plane length scale associated with the roughness increases as a power law with multilayer thickness. It is suggested that the loss of conformality, characterized by a relatively short out-of-plane correlation length, may be the cause of the reduction in anisotropy energy per interface observed for high numbers of bilayer repeats. There is a weak association between fractal parameter and interface anisotropy; a reduction in the fractal dimension of the interface appears to result in a higher surface anisotropy.

(Some figures in this article are in colour only in the electronic version)

1. Introduction

A strong perpendicular magnetic anisotropy (PMA) is observed in Co/Pd multilayers. It can be strong enough to lift the magnetization out of the layer plane when the thickness of the Co layer is less than ∼8 Å [1], and there has been much work on the system as a possible high density recording medium. Although it is well established that the perpendicular anisotropy is associated with the interface structure, recent work suggests that the mechanism of surface anisotropy originally suggested by Néel is inadequate. Interface roughness [2], and the degree of mixing of the atoms at the interface [3], have been predicted to affect the anisotropy. Palasantzas *et al* [4] and Macrander *et al* [5] examined the effect of roughness on coercivity,

[3] Permanent address: Nanophysics Research Group, Center for Nanosciences and Nanotechnologies, University of Isfahan, Isfahan, 81746-73441, Iran.

domain wall width, and domain size. They suggested that a precise determination of film roughness as well as its growth mechanism using x-ray and electron diffraction is a necessary step in correlating microstructural disorder with magnetic properties.

The effect of layer structure on magnetic properties of Co/Pd multilayers has been studied by several authors [6–8], with particular emphasis on the effect of buffer layers [9, 10]. An enhancement of coercivity by underlayer control in Co/Pd multilayers has been reported by Oh and Joo [11], who found that the coercivity of Co/Pd multilayers was strongly dependent on the sputtering pressure of the underlayer and could be increased by increasing the sputtering pressure of the Pd underlayer. Kim *et al* [12] studied the interfaces of Co/Pd multilayers by polarized extended x-ray absorption fine structure analysis and observed the presence of a Co–Pd alloy-like phase at the interface. In a more recent paper, Kim and Shin [13] reported that the alloy-like character is dominant at interfaces in typical Co/Pd multilayers and yields PMA through the strain anisotropy of Co atoms. They found that the broken symmetry, generally considered as the origin of PMA, was not definitely necessary for the presence of PMA in Co/Pd multilayers.

In this paper, we examine how the number of bilayer repeats in sputtered Co/Pd multilayers affects both the magnetic properties and the interface structure revealed by grazing incidence x-ray scattering.

2. Experimental and data analysis details

Two series of {Pd 30 Å/(Co xÅ/Pd 30 Å) $\times$ N} multilayer films were grown on single-crystal (001) oriented silicon using the magnetron sputtering technique at the University of Leeds. The initial Pd layer acted as a buffer to the native oxide on the silicon surface.
Series 1: Si/SiO_2/30 Å Pd/N $\times$ {5 Å Co/30 Å Pd} where $N = 2, 4, 6, \ldots, 30$.
Growth conditions: 3 mTorr Ar; Co 100 mA, 33 W; Pd 50 mA, 17 W.
Series 2: Si/SiO_2/30 Å Pd/N $\times$ {8 Å Co/30 Å Pd} where $N = 2, 4, 6, \ldots, 30$.
Growth conditions: 3 mTorr Ar; Co 100 mA, 34 W; Pd 50 mA, 17 W.
(Further results relating to two other similar series may be found in [14].)

All magnetic measurements were performed at room temperature, anisotropy measurements being obtained by recording in-plane and out-of-plane M–H loops using a vibrating sample magnetometer. (While the magnetic properties were measured for most of the samples studied by x-ray scattering, this was not always the case.) Most of the x-ray experiments were carried out on a Bede GXR1 laboratory reflectometer and on station 2.3 at the SRS (Daresbury, UK). A few of the measurements were made at the XMaS beamline, BM28, at the ESRF, Grenoble. All synchrotron radiation measurements were made in the incidence plane with a wavelength 1.3 Å, a 5 mm slit integrating the scatter over a small range of wavevector out of the incidence plane. The geometry and data collection procedures are standard and well documented elsewhere [15].

Structural parameters were obtained by fitting the observed x-ray scattering distribution to that simulated from a model structure. Values of thickness and interface width were first found by automatic refinement of the specular scatter using the Bede REFS MERCURY code [16], and these parameters then used to fit the diffuse scatter using the code manually. A co-refinement process was adopted to determine the topological roughness σ, in-plane correlation length ξ, the out-of-plane correlation length ζ and the interface Hurst fractal parameter h. Any trial structure was tested against at least three diffuse scatter distributions taken at different scattering vectors, the model adopted being that which gave a minimum difference over all data sets.

The Bede REFS code [17], which has been used to fit the diffuse scatter, is based on a self-affine fractal description of the interfaces within the distorted wave Born approximation

(DWBA). It incorporates the conformal propagation of roughness through a multilayer in one of two ways. The first (model 1) is to assume that there is a constant 'vertical' correlation fraction (VCF) of the conformal to the non-conformal roughness. Within this model there is a single in-plane correlation length ξ and fractal parameter h defining the height to height correlation function, and the relative amount of conformal and non-conformal roughness is constant for every layer in the multilayer stack. This is computationally rapid, and computation time scales as the number of layers. The second model (model 2) assumes that, at the bottom of the multilayer, all the roughness is conformal but that the non-conformal fraction increases with the interface number. This is incorporated by assuming an exponential decay of the conformal fraction, the decay length being the out-of-plane correlation length ζ. The second model is more physically realistic, but the computation time scales as the square of the number of layers. Both models make the very drastic assumptions that all roughness frequencies propagate with the same out-of-plane correlation length and that the in-plane correlation length does not change from one layer to the next.

3. Results

3.1. Magnetic measurements

All samples of series 1 showed perpendicular anisotropy, the easy direction lying out of the multilayer plane. The value of the effective anisotropy K_{eff}, which includes the magnetostatic, magnetocrystalline and interface anisotropies, normalized to the magnetic volume, derived from the area between the in-plane and out-of-plane M–H loops is shown for the series 1 samples as a function of bilayer repeats in figure 1(a). The 20 bilayer sample had a maximum value of $K_{\mathrm{eff}} = (3.0 \pm 0.2)$ Merg cm^{-3}. In the out-of-plane measurements all samples were found to have low coercivity (figure 1(b)), a feature often noted in sputtered Co/Pd multilayers [18], although it has also been reported for multilayers grown by other techniques [19]. This may be associated with the formation of the stripe domain state. For the series 2 samples, with thicker Co layers, in-plane magnetization was found for fewer than 10 bilayer repeats. Perpendicular anisotropy was observed for all samples with a greater number of repeats.

3.2. X-ray measurements

Low-angle Bragg peaks arising from the Co/Pd layer periodicity were identifiable in the specular reflectivity profiles of samples with more than 4 bilayer repeats. From the spacing and relative heights of the successive orders of Bragg reflection, we can obtain a measure of the thickness of the repeated layers. However, in order to obtain a good fit between simulated and experimental specular profiles in the region between the Bragg peaks, the first two layers were taken as buffer layers of significantly different composition and interface width. Using the model structure shown in figure 2, a good fit between simulation and experiment was achieved in all cases, an example being shown in figure 3. The limit on the statistical difference between simulation and experiment enables us to determine the layer thickness and interface width to a precision of 0.3 Å (table 1).

Also shown in figure 3 is the diffuse scatter recorded in a coupled detector–specimen scan with the specimen offset 0.1° from the specular condition. Such a scan measures the diffuse scatter just below the specular ridge, the interference fringes coming from diffuse scatter coherent between the top and bottom of the multilayer. These off-specular Kiessig fringes provide a measure of the conformality of the roughness between the bottom and top

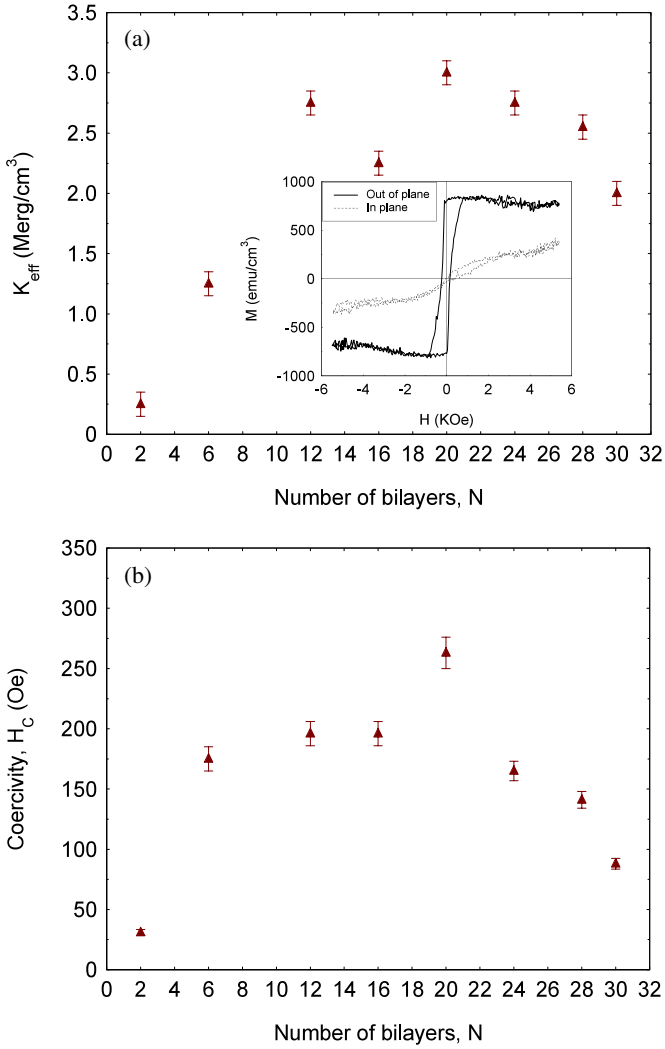

Figure 1. Relation between number of bilayers and (a) K_{eff}, and (b) coercivity. (The inset to (a) shows the in-plane and out-of-plane hysteresis loops for the 12 bilayer sample, series 1.)

of the multilayer stack. Figure 4 shows the off-specular diffuse scatter for different number of bilayer repeats. We note that the Kiessig fringes disappear at about 16 bilayers, indicating $\zeta \approx 400$ Å. The retention of the off-specular Bragg peaks indicates that the conformality between successive layers is retained to the largest number of repeats studied. The diffuse scatter is best studied by scanning the scattering vector tip in the direction of the surface, a so-called transverse scan. This is achieved by rocking the sample for fixed detector position. An example of such diffuse scatter profiles for different detector angles (scattering vector magnitude) is given in figure 5. The simulated lines correspond to the one set of model parameters (listed in table 1) that gives the best overall fit to all four scans.

Examination of the diffuse scatter, as a function of specimen angle with the detector set at the first multilayer Bragg peak (figure 6), shows strikingly how the diffuse scatter distribution changes with increase in bilayer repeat number N. As N increases, so the scatter becomes

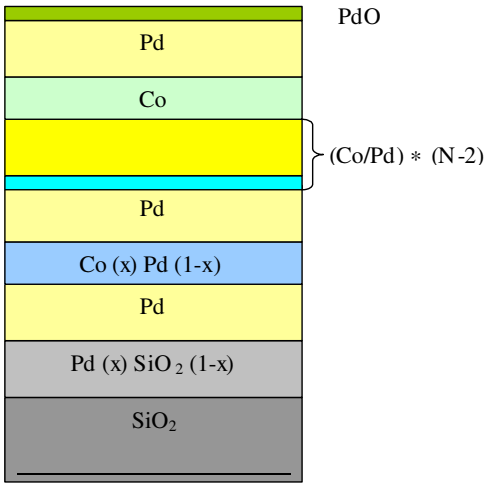

Figure 2. Model structure used to refine x-ray data.

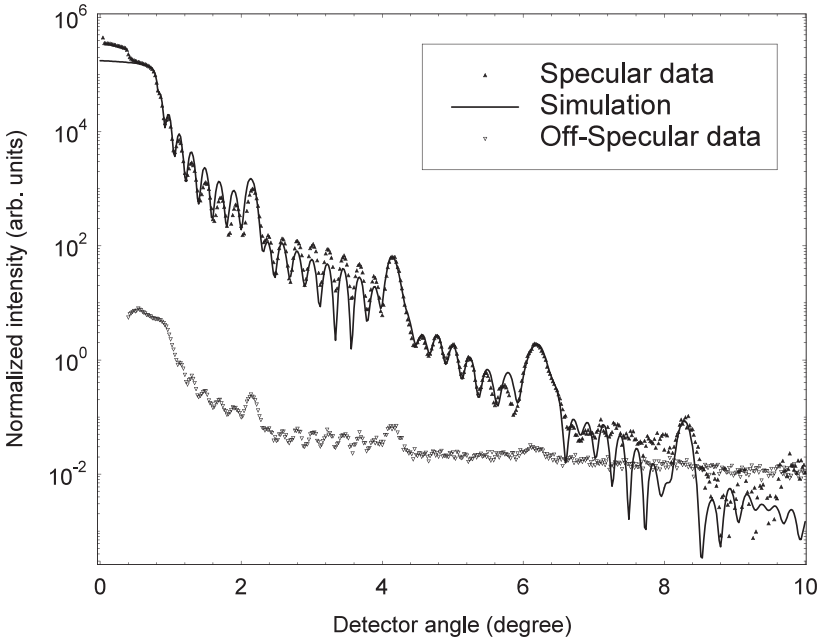

Figure 3. Specular and off-specular scatter from an 8 bilayer sample. (The discrepancy between simulated and experimental specular data at very low angle arises from second-harmonic ($\lambda/3$) contamination in the beam from the monochromator.)

more concentrated towards the specular ridge, a feature characteristic of an increasing in-plane correlation length. The variation of the in-plane correlation length, derived from the best-fit parameters to the diffuse data sets, is plotted in figure 7 for sample series 1 and 2. A similar rise is found in the other two series.

The dependence of the out-of-plane correlation length ζ on N is not strong, though in series 1 there is a suggestion of an upwards trend. Figure 8 shows the variation of ζ with N for

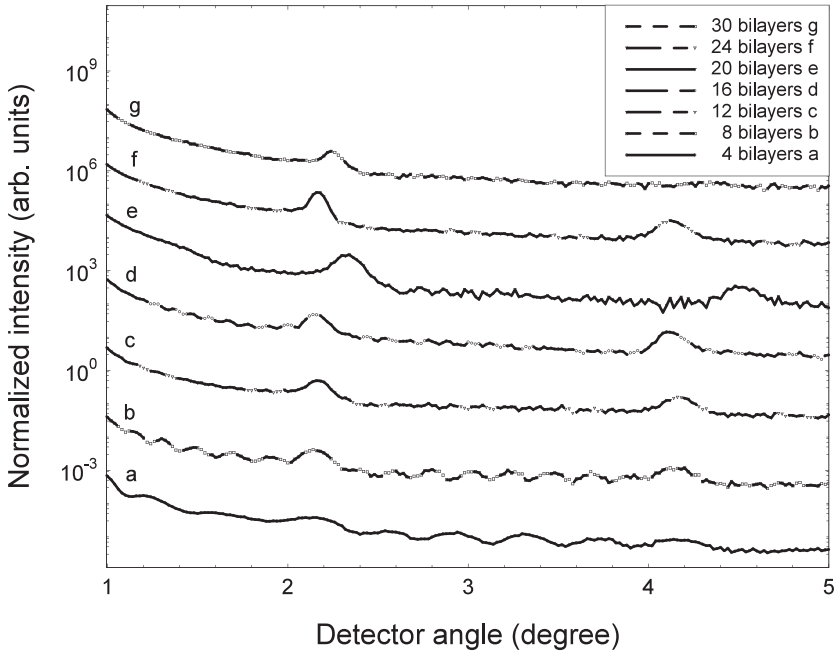

Figure 4. Off-specular diffuse scatter as a function of detector angle for increasing bilayer number. (N increases up the figure; successive curves are offset for clarity.)

Table 1. Layer and interface parameters derived from the refinement of x-ray data.

N	t_{Buffer} ±0.3 Å	t_{Co} ±0.3 Å	t_{Pd} ±0.3 Å	σ_{Buffer} ±0.3 Å	σ_{Co} ±0.3 Å	σ_{Pd} ±0.3 Å	VCF	ζ (Å) ±10%	ξ (Å) ±10%	h ±10%
4	33.5	5.7	29.4	4.0	5.0	3.2	0.3	80	40	0.50
8	29.6	5.8	30.2	6.1	3.1	3.8	0.3	200	60	0.40
12	27.2	6.5	29.5	4.7	2.9	3.4	0.2	160	100	0.60
16	39.6	6.4	30.6	4.2	6.2	3.0	0.2	200	200	0.50
20	31.5	4.9	28.7	7.3	4.2	8.9	0.2	200	300	1.00
24	39.9	4.0	32.9	8.3	3.6	11.0	0.1	250	500	0.70
26	39.3	5.0	31.7	6.9	10.8	5.5	0.1	250	600	0.60
30	26.7	1.5	33.8	8.7	4.1	5.2	0.05	250	900	0.75

sample series 1. If the point corresponding to $N = 4$ is neglected, the change with increasing N is small. (The total thickness of the $N = 4$ multilayer is less than 200 Å, making the value of ζ obtained through fitting of the diffuse scatter to model 2 in the Bede REFS code physically unreliable.) For all other series, ζ remains constant within each series and is between 200 and 300 Å [14]. For all sample series there is a drift upwards in h, towards a more two-dimensional fractal interface, as a function of N (figure 9).

4. Discussion

The perpendicular anisotropy, normalized to the number of interfaces or magnetic volume, represented by K_{eff}, might be expected to remain constant with the number of bilayers N, that is the number of interfaces. However, as for Co/Pt multilayers [20, 21], there is a maximum

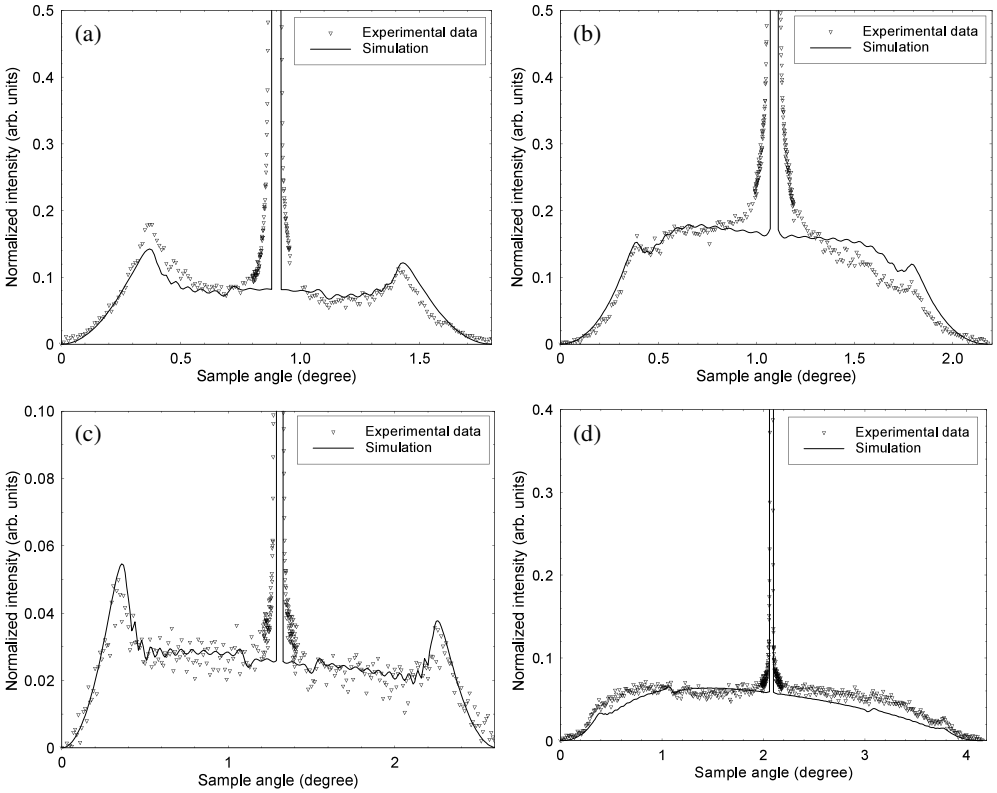

Figure 5. Example of the co-minimization of the fit to the diffuse scatter for the 12 bilayer sample. Detector angles (a) 1.8°, (b) 2.18°, cutting first Bragg sheet (c) 2.62° (d) 4.16°, cutting second Bragg sheet. (The full-width half-height maximum of the specular ridge is $0.016 \pm 0.001°$; the features seen are associated with diffuse scatter.)

in K_{eff} for these Co/Pd samples at about $N = 20$ (figure 1(a)). The variation is, however, less marked than for Co/Pt. Nevertheless, the rise and fall does suggest that changes to the interface structure may be occurring. The total layer thickness for $N = 20$ is about 700 Å and inspection of figures 7–9 indicates that there is no obvious structural parameter that corresponds specifically to this thickness. However, by that thickness, almost all the conformality in the roughness has been lost between the bottom and the top of the multilayer stack. The modelling suggests that the roughness on top of the Co layers stays almost constant as the bilayer repeat number N increases, there being a small increase in the roughness amplitude on the top of the Pd layers. As the conformality between the bottom and the top of the stack has been lost in the layers with large N, this increased roughness must be predominantly non-conformal. The random nature of such interface fluctuations may be expected to reduce the strength of the interface anisotropy. There is an associated fall in coercivity (figure 1(b)), which may be associated with enhanced ease of domain wall nucleation due to the roughness.

The ability to fit the diffuse scatter with the value of the interface width derived from the specular scatter (figure 3) indicates that the intermixing at the Co and Pd interfaces within the majority of the multilayer stack is very small. As large real space length scales correspond to short distances in reciprocal space, a large in-plane length scale results in concentration of the diffuse scatter in transverse scans close to the specular peak. Conversely, a short in-plane

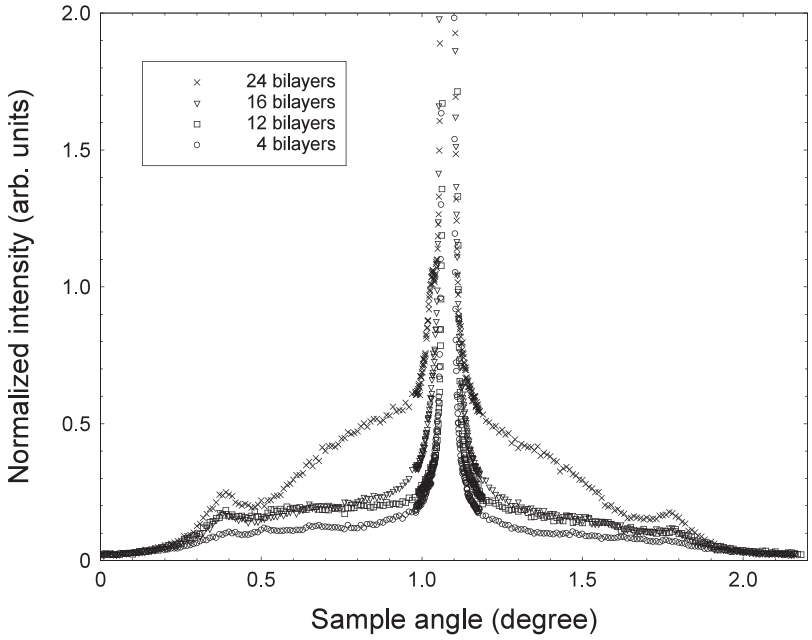

Figure 6. The diffuse scatter through the first multilayer Bragg peak for different bilayer repeat number N.

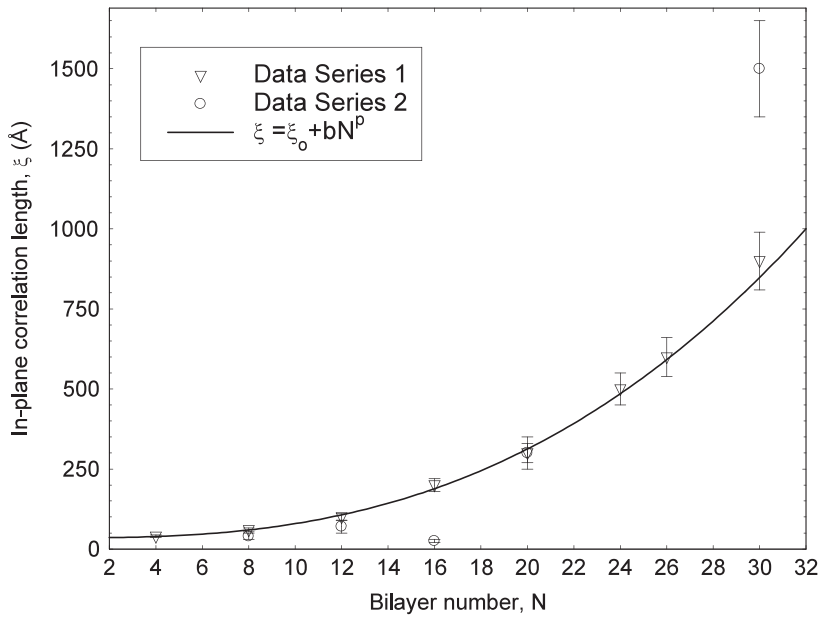

Figure 7. In-plane correlation length ξ as a function of bilayer number N for sample series 1 (triangles) and series 2 (circles). The solid line is a fit to the series 1 data points.

correlation length results in the scatter being spread much more uniformly and over a wider range of reciprocal space. The traces shown in figure 6, taken through the first multilayer Bragg

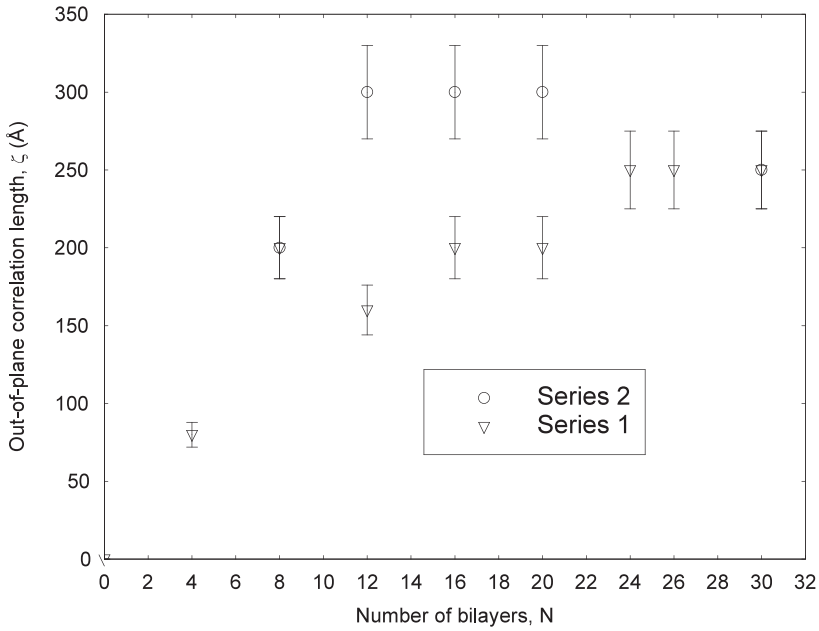

Figure 8. Variation of the out-of-plane correlation length ζ as a function of N for samples of series 1 (triangles) and series 2 (circles).

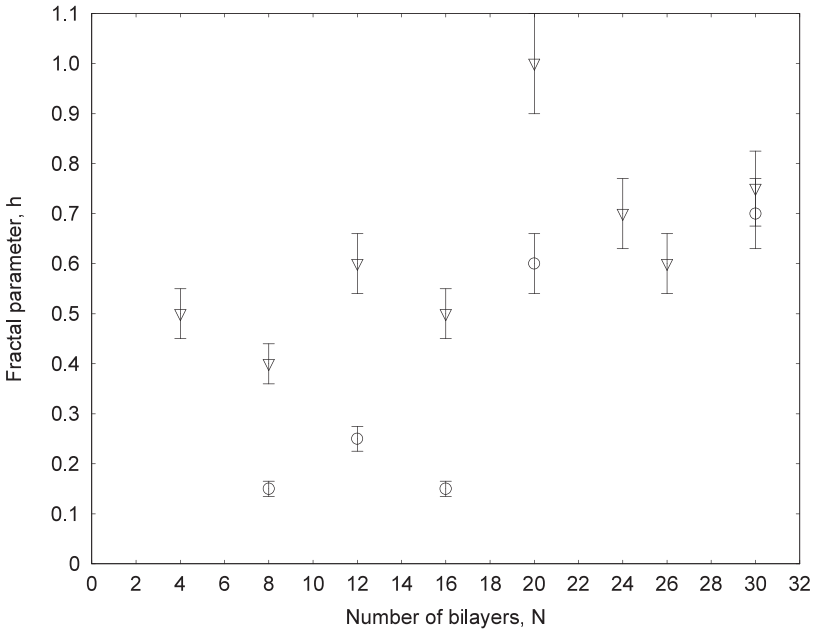

Figure 9. Variation of fractal parameter h as a function of N for samples of series 1 (triangles) and series 2 (circles).

peak, demonstrate that the in-plane length scale is increasing with increasing N. Detailed fitting of the diffuse scatter confirms this observation, model 2 within the REFS code (shown

in figure 5) giving much better fits than model 1. We find that the in-plane correlation length increases significantly with bilayer number. Such behaviour is consistent with the predictions of Tang, Alexander and Bruinsma in the so-called TAB model [22] of layer growth, which takes a Huygens construction approach to roughness propagation. The model, which has been tested successfully against experimental data from W/Si multilayers [23], predicts columnar growth and that low frequencies propagate much more readily than high-frequency roughness components. The model predicts that in late stage growth of a single layer the in-plane correlation length ξ should scale as thickness t^p where the exponent $p = 0.75$. Earlier in growth from a buffer that has a smaller value of h, i.e., has a more three-dimensional nature to the roughness, $p < 0.75$. With the modification of a small constant component to the correlation length ξ_o, the in-plane correlation length ξ obeys power law dependence on the bilayer number (thickness) well (figure 7). However, for series 1 the scaling exponent is 2.8 ± 0.2, very much larger than that predicted by the TAB or any other growth models. (For series 2 alone, the exponent is even higher at 4.2 ± 0.1, but the fit is dominated by one very high data point at $\xi = 1500$ Å. Without this point, a single curve fits the series 1 and 2 data.) At present we do not have an explanation for this discrepancy, but note that the x-ray measurement averages over the depth of the multilayer; Kiessig fringes are observed in the specular scatter close to the Bragg peaks for all the samples, showing that the x-ray wave penetrates to the bottom of the multilayer. In fitting the data we average over all frequencies of roughness and assign a single correlation length to the multilayer roughness, including the buffer layer. The increase in ξ with N represents a loss of high-frequency roughness components as the multilayer grows. We note that if model 1 is used (table 1), the vertical correlation fraction (VCF) necessary to get a reasonable fit falls linearly as N increases. Within this model, multilayers with $N = 24$ and 30 have only 10% and 5% of the whole roughness conformal (table 1). Thus, for the thicker multilayers, the majority of the roughness is random. This development is consistent with the relatively short out-of-plane correlation length ζ determined from fits to model 2 (figure 9). Although there is a modest increase with N shown here for sample series 1, there is no significant variation with N for the other series. However, the values of ζ are remarkably similar between the series. Thus for the multilayers with large values of N, there is conformality on a short length scale over a few repeats but no conformality between the lower and upper layers. Within the TAB model, this is represented by shadowing of adjacent columns in the columnar growth mode, the laterally shadowed grains losing the conformality with the material below. This growth mode can be effectively described by an increase in the in-plane correlation length for the overall roughness, the REFS model only accommodating a single in-plane length scale for all types of roughness. The exponent will not correspond to the frequency-dependent exponents derived from the TAB or other growth models [24, 25].

Table 1 shows that multilayers with large numbers of repeats tend to have larger value of the fractal parameter h than those with few repeats. As N rises, and with it ξ, so the interfaces become more two dimensional in character, i.e., h tends to 1. This is consistent with the preferential loss of the high-frequency components of the roughness. There is a weak correlation between the fractal parameter h and the magnetic anisotropy K_{eff} (figure 10). Such behaviour was also found for sputtered Co/Pt multilayers [21].

5. Conclusions

There is evidence that the interface structure in sputtered Co/Pd multilayers develops a longer in-plane length scale to the roughness as the number of multilayer repeats increases. For large values of N, the roughness is predominantly non-conformal and is approximately described by a two-dimensional fractal interface. As the non-conformal, two-dimensional fractal character

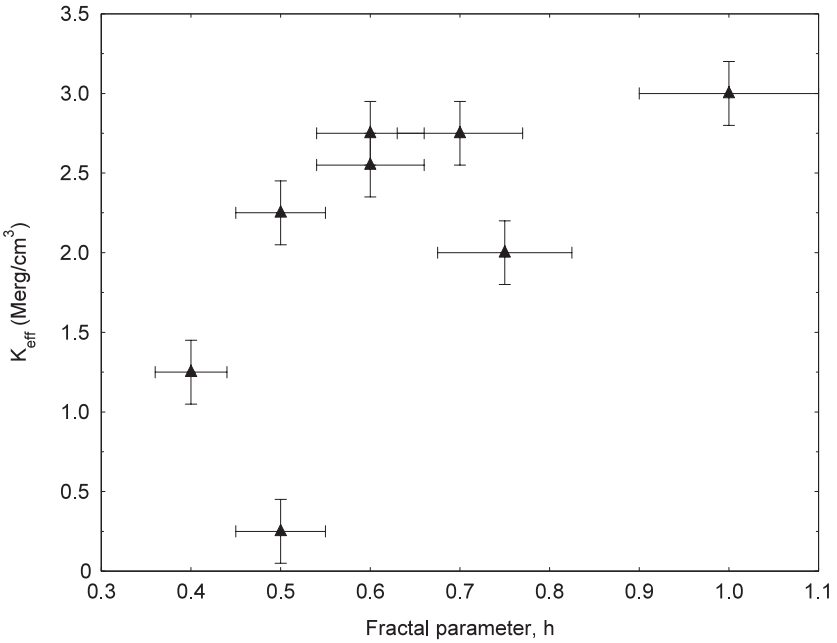

Figure 10. Effective anisotropy, normalized to magnetic volume, as a function of fractal parameter for sample series 1.

develops, the anisotropy energy per interface drops, suggesting that conformal roughness is important in the development of perpendicular anisotropy. As the fraction of conformal roughness falls, so does the anisotropy energy per interface. The reduction in the interface fractal dimension shows a weak correlation with the perpendicular magnetic anisotropy energy per interface. As with Co/Pt, there is a suggestion that interfaces that have more nearly three-dimensional character ($h \rightarrow 0$) have a lower interface anisotropy than those more nearly two-dimensional in nature ($h \rightarrow 1$).

Acknowledgments

Support from the beamline staff at the Daresbury SRS XMaS and at the beamline in Grenoble is gratefully acknowledged. The project was supported financially by EPSRC and the Government of Iran.

References

[1] den Broeder F J A *et al* 1987 *J. Appl. Phys.* **61** 4317
[2] Bruno P 1988a *J. Phys. F: Met. Phys.* **18** 1291
Bruno P 1988b *J. Appl. Phys.* **64** 3153
[3] den Broeder F J A *et al* 1988 *Phys. Rev. Lett.* **60** 2769
[4] Palasantzas G *et al* 2000 *Physica* B **283** 199
[5] Macrander A T *et al* 2000 *Physica* B **283** 157
[6] Roy A G *et al* 2001 *J. Appl. Phys.* **89** 7531
[7] Asahi T *et al* 2001 *J. Magn. Magn. Mater.* **235** 87
[8] Ohmori H and Maesaka A 2001 *J. Magn. Magn. Mater.* **235** 45
[9] Onoue T *et al* 2002 *J. Appl. Phys.* **92** 4545

[10] Kawaji J *et al* 2002 *J. Magn. Magn. Mater.* **251** 220
[11] Oh H S and Joo S K 1996 *IEEE Trans. Magn.* **32** 4061
[12] Kim S K *et al* 1997 *J. Magn. Magn. Mater.* **170** L7
[13] Kim S K and Shin S C 2001 *J. Appl. Phys.* **89** 3055
[14] Rozatian A S H 2004 *PhD Thesis* University of Durham
[15] Pape I *et al* 1998 *Physica* B **253** 278
[16] Wormington M *et al* 1999 *Phil. Trans. R. Soc.* A **357** 2827
[17] Wormington M *et al* 1996 *Phil. Mag. Lett.* **74** 211
[18] Yamane H *et al* 1993 *J. Appl. Phys.* **73** 334
[19] Kudo K *et al* 2001 *Electrochim. Acta* **47** 353
[20] Greaves S J *et al* 1993 *J. Magn. Magn. Mater.* **121** 532
[21] Rozatian A S H *et al* 2003 *J. Magn. Magn. Mater.* **256** 365
[22] Tang C *et al* 1990 *Phys. Rev. Lett.* **64** 772
[23] Salditt T *et al* 1996 *Europhys. Lett.* **36** 565
[24] Karder M *et al* 1986 *Phys. Rev. Lett.* **56** 889
[25] Edwards S F and Wilkinson D R 1982 *Proc. R. Soc.* A **381** 17